nature communi ns

mechanisms. A recent global study has detected a subtle increase in RH in northern peatlands over the last four decades[17] (Supplementary Fig. 1), suggesting that the actual water vapor (AVP) increases at approximately the same rate as the saturation water vapor (SVP) ($RH = f(AVP, SVP)$). This may be due to the unique surface characteristics of the water-rich environment and the high moss cover in the northern peatlands, which supplies sufficient atmospheric water to meet the increasing water demand caused by high VPD[18] and to maintain the atmospheric water balance. If RH remains unchanged, =

Vegetation responses to rising VPD caused b concurrent warming and decreasing RH in global nonpeatland regions

Increasing VPD caused by concurrent warming and decreasing RH led to a stronger suppression impact on GPP in global nonpeatland regions. Ta (mean ± 1 se, 0.027 ± 0.003 °C yr^{-1}, $p < 0.001$) and VPD (0.018 ± 0.001 hPa yr^{-1}, $p < 0.001$) increased significantly during 1982–2018, but RH (−0.027 ± 0.005% yr^{-1}, $p < 0.001$) decreased significantly in global nonpeatland regions (Fig. 3a–c). From 1982 to 2018, ~60% of the global nonpeatland regions showed an increasing VPD trend with significantly increasing Ta and significantly declining RH ($p < 0.05$, Supplementary Fig. 4). When the detrended Ta, radiation,

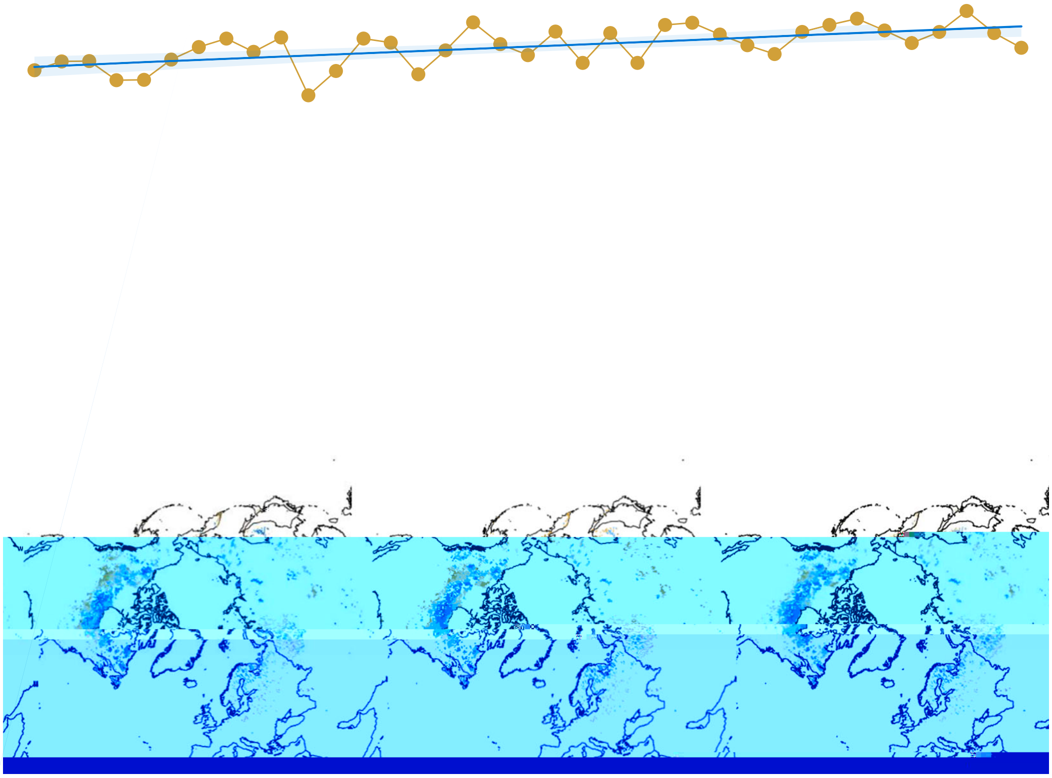

nonpeatland regions (44.3–58.2% with a significant negative correlation, $p < 0.05$) (Fig. 3d, Supplementary Fig. 5). The regional mean $PCOR_{GPP\ vs.\ VPD}$ ranged from −0.16 to −0.21 for the three satellite-derived GPP (Fig. 3d). The spatial coverage of significantly negative $PCOR_{GPP\ vs.\ VPD}$ was 40% higher and the regional mean $PCOR_{GPP\ vs.\ VPD}$ was 0.25 lower in the global nonpeatland regions than those in the northern peatlands (Fig. 3d).

To further assess the robustness of the divergent drivers and impacts of increasing VPD, the global nonpeatland regions were divided into nonhumid regions (AI < 0.65) and humid regions (AI ≥ 0 [illegible] based on the aridity index (AI, Methods)[31]. From 1982 to 20 [illegible] in the temporal trends of Ta, RH, and VPD in the no [illegible] the humid regions were consistent with th [illegible] land region (Supplementary Figs 4 [illegible] detrended Ta, radiation [illegible]

considered, showed that the spatial coverage of significantly [illegible] $PCOR_{GPP\ vs.\ VPD}$ were 59.5% higher (mean of the thre [illegible] GPP) in the nonhumid regions and 25.4% grea [illegible] respectively ($p < 0.05$, Supplementar [illegible] northern peatlands. In additio [illegible] from three satellite-d [illegible] regions (−0.3 [illegible] norther [illegible] the northern [illegible] were validated by [illegible] eddy covariance flux towers. [illegible] detrended VPD was significantly [illegible] detrended GPP at 1 out of 18 (5.6%) eddy [illegible] towers in the northern peatlands and 43 out of 95 [illegible] towers in global nonpeatland regions, respectively ($p < 0.05$,

Fig. 3d). Grouping the 95 eddy covariance flux towers into the nonhumid regions (33 towers) and the humid regions (62 towers) further confirmed a greater VPD suppression impact in the global nonpeatland regions compared to the northern peatlands, with a significantly negative $PCOR_{GPP\ vs.\ VPD}$ of 63.6% and 35.5% in the nonhumid regions and the humid regions, respectively (Supplementary Fig. 6). In addition, according to the latitude, longitude, and time span in 113 eddy covariance flux towers, we found that the symbols (±) of the satellite-derived $PCOR_{GPP\ vs.\ VPD}$ agreed with 76.4% (mean value from three satellite-derived GPP) of the eddy covariance flux towers (Supplementary Fig. 7, Methods). In addition, the satellite-derived $PCOR_{GPP\ vs.\ VPD}$ was positively correlated with eddy covariance $PCOR_{GPP\ vs.\ VPD}$, with r values ranging from 0.51 to 0.58 ($p < 0.05$, Supplementary Fig. 7). In summary, the field-scale and grid-scale observations consistently suggested that the prevailing viewpoint derived from the global nonpeatland regions may overestimate the VPD suppression impact in the northern peatlands.

Mechanisms for the divergent VPD effects

Six plant traits and environmental factors were used to understand the causes of the contrasting VPD effects. Soil hydraulic properties were

H_2O lower and 0.22 higher than the global nonpeatland regions, respectively (mean ± 1 se, 1.23 ± 0.01 vs. 1.84 ± 0.01 g C $kPa^{0.5}$ kg^{-1} H_2O, 0.13 ± 0.01 vs. −0.09 ± 0.006) (Fig. 4c). Overall, plants in the northern peatlands tended to adopt an "open" water-use strategy with lower uWUE and higher $PCOR_{Et\ vs.\ VPD}$ in response to increasing VPD, leading to a weaker suppressive impact on vegetation growth compared to the global nonpeatland regions.

We further assessed the robustness of the satellite-derived differences in the plant traits between the northern peatlands and the global nonpeatland regions using eddy covariance flux towers. As the proxy for the plant water-use strategy, the uWUE in the northern peatlands was 0.78 g C $kPa^{0.5}$ kg^{-1} H_2O lower than that in the global nonpeatland regions (mean ± 1 se, 1.10 ± 0.12 vs. 1.88 ± 0.10 g C $kPa^{0.5}$ kg^{-1} H_2O) (Fig. 4c). Compared to the global nonpeatland regions, weak stomatal regulation and an abundant atmospheric water supply in response to increasing VPD in the northern peatlands were also confirmed by the eddy covariance flux datasets. For stomatal activity, a significant negative response of *Gc* to VPD was found in only 5.6% of the eddy covariance flux towers in the northern peatlands (coefficient mean ± 1 se, 0.04 ± 0.08), whereas this percentage increased to 52.6% in the global nonpeatland regions (− 0.27 ± 0.04) ($p < 0.05$, Fig. 4c, Methods). As a proxy for atmospheric water supply with increasing VPD, a significant negative response of evapotranspiration (ET) to VPD

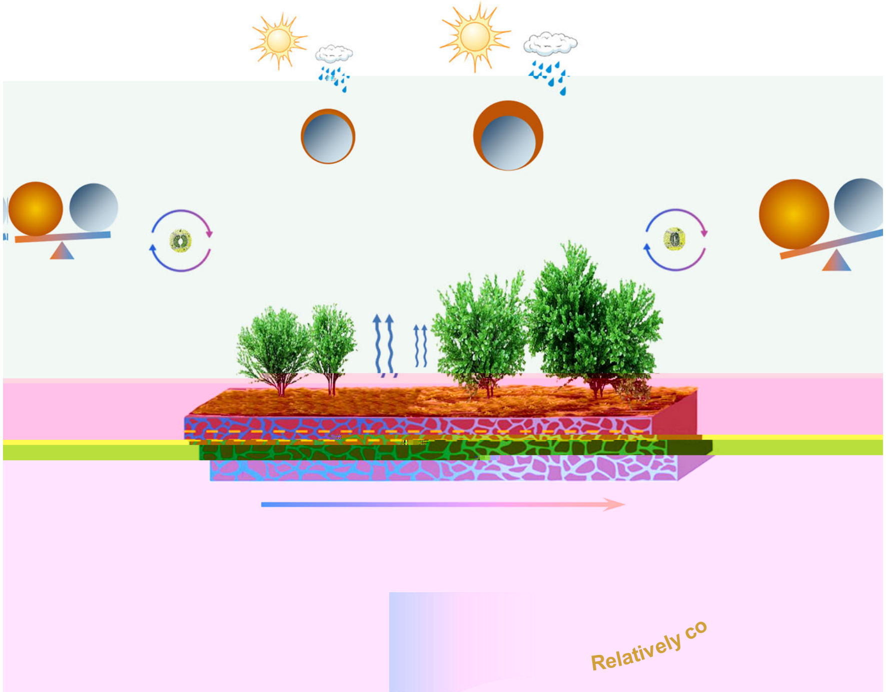

increased with increasing VWC and SOC, but it decreased with increasing BD and CWD (Fig. 4b). Compared to the global nonpeatland regions, higher VWC (mean ± 1 se, 17.58 ± 0.12 vs. 13.56 ± 0.02%) and SOC (1.11 ± 0.02 vs. 0.26 ± 0.002%) and lower BD (1.06 ± 0.01 vs. 1.30 ± 0.001 g m^{-3}) and CWD (15.9 ± 0.20 vs. 37.4 ± 0.20 mm) were observed in the northern peatlands (Fig. 4c). These differences suggested that vegetation in the northern peatlands with good soil hydraulic properties and abundant water availability could resist the atmospheric water stress caused by increasing VPD compared to the global nonpeatland regions.

We then assessed the cascading correlations of plant water-use strategy, water availability, and soil hydraulic properties with VPD effects using mediation effect models (Methods). The results showed that the water availability and the soil hydraulic properties significantly influenced the VPD effects by determining the plant water-use strategy ($p < 0.05$, Fig. 4d, e). Specifically, changes in VWC (standardized indirect effect ± 1 se from three datasets of satellite-derived GPP, 0.14 ± 0.001) and SOC (0.15 ± 0.001) had a significant positive indirect effect on $PCOR_{GPP\ vs.\ VPD}$ through decreasing uWUE and increasing $PCOR_{Et\ vs.\ VPD}$ ($p < 0.05$, Fig. 4d, e). In contrast, a significant negative indirect effect was observed from changes in CWD (− 0.26 ± 0.01) and BD (− 0.18 ± 0.001) ($p < 0.05$, Fig. 4d, e). Collectively, compared to the global nonpeatland regions, plants in the northern peatlands adopted an "open" water-use strategy in response to increasing VPD because of the wet environment, favorable soil hydraulic properties, and adequate atmospheric water supply, resulting in a neutral response of vegetation growth to increasing VPD.

Implications

This study represents one of the first attempts to mechanistically examine the VPD impacts on vegetation growth in northern peatlands. The neutral response of vegetation growth to warming-induced increasing VPD in the northern peatlands (Fig. 5) suggested that the prevailing views of vegetation suppression under increasing VPD are not necessarily the case across the globe. This can be explained by the fact that plants in the wet soil–air environment of the northern peatlands tended to adopt an "open" water-use strategy by relaxing stomatal regulation to maximize carbon uptake even as VPD increases (Fig. 5).

An ample atmospheric water supply, driven by a water-rich environment and high moss cover, was a critical factor in determining whether the increasing VPD was caused by warming alone in the northern peatlands. Factors contributing to the wet environment (e.g., relatively high VWC and low CWD) were the high water table[43], snow melt[44], permafrost thaw[45], and good soil hydraulic properties (e.g., relatively low BD and high SOC), which could directly accelerate water movement from the underlying surface into the atmosphere to meet the increasing water demand caused by rising VPD[28] in the northern peatlands. A high moss cover is another essential contributor to the atmospheric water supply with increasing VPD in the northern peatlands[18]. Mosses can store substantial water in their interconnected cavernous structures[46], yet they fail to minimize water loss under increasing atmospheric water demand due to a lack of stomatal regulatory structures[47,48]. Combining these characteristics with a large surface area, the water evaporation rate in moss is even higher than in open water[47]. Under the same environmental conditions, our synthesized observations showed that the ET of moss was significantly greater by 0.43 ± 0.14 mm day^{-1} (mean ± 1 se) than that of vascular plants ($p = 0.009$, Supplementary Fig. 9). The moss-dominated wet system of the northern peatlands allowed ET and Et to increase with increasing VPD[18]. Therefore, a sufficient atmospheric water supply allowed increases in AVP in approximately the same proportion as the SVP, leading to increasing VPD induced by warming alone in the northern peatlands.

A neutral response of vegetation growth to warming-induced increased VPD was observed in the northern peatlands. This is contrary to the prevailing views that increasing VPD induced by the coaction of warming and decreased RH markedly depressed vegetation growth in global nonpeatland regions[6–10,22,49]. A relatively dry environment in the global nonpeatland regions can limit atmospheric water supply under increasing VPD, disrupting the supply-demand balance of atmospheric water conditions and exacerbating atmospheric water stress[27]. This can increase the hydraulic burden of plants, limiting their stomatal activity to preventing excessive water loss at the expense of photosynthesis[16,50]. In contrast, the moss-dominated wet system of the northern peatlands can provide adequate atmospheric water to meet the increased water demand caused by increasing VPD. Even if atmospheric water stress occurs as warming-induced VPD increases, the stress may be below the threshold that leads to stomatal closure, as evidenced by the neutral response of *Gc*, Et, and GPP to increasing VPD. In this wet soil–air environment, plants adopt an "open" water-use strategy in response to water stress, maximizing carbon uptake by relaxing stomatal regulation[24,29]. Although an "open" water-use strategy may sacrifice hydraulic security, plants in water-rich environments would benefit more from keeping their stomata open to take up carbon than from conserving water[29,41]. Multisource datasets consistently demonstrated that plants in the northern peatlands were believed to

The warming experiment at the Mohe site was conducted in a peatland in the northern Greater Hinggan Mountains (Tuqiang Forestry Bureau in Mohe city, Heilongjiang Province; 52.93°N, 122.83°E). The peatland is characterized by a humid monsoon climate in a cold temperate zone with a mean annual temperature and precipitation of −3.9 °C and 450 mm, respectively. The growing season lasts for *c.* 120 days, from mid-May to mid-September. Four common native plant species in the plant community are *Sphagnum palustre* (SP), *Vaccinium uliginosum* (VU), *Ledum palustre*

The flux tower-based GPP, latent heat flux (LE, W m^{-2}), sensible heat flux (H, W m^{-2}), and environmental variables of Ta, VPD, precipitation, shortwave radiation, wind speed (m s^{-1}), friction velocity (u_8, unitless), and atmospheric pressure were obtained from the global eddy-covariance flux dataset, FLUXNET2015 (global nonpeatland regions) and FLUXNET-CH_4 Community Product (northern peatlands). Following recent studies on VPD effects, we used GPP estimates based on the nighttime partitioning method (i.e., "GPP_NT_VUT_REF")[7,20]. We identified and used sites with at least 3 years (more than 15 months) of high-quality data (≥75% of good quality data in a month)[63]. In addition, we removed all cropland towers in the study area to exclude the effects of human activity[7] and the mean r was >0.8 in this study. In the analyses, one of the predictor variables was perturbed by one standard deviation (a value of 1 due to the initial input data normalization), and $PCOR_{GPP\ vs.\ VPD}$ was predicted again using the existing random forest model with the pre-

31. [illegible] Nat. Ecol. Evol. **4**, 10 [illegible] –10[illegible] (2020).
32. [illegible] J. Adv. Modeling Earth Syst. **6**, 24 [illegible] (2014).
33. [illegible] Earth-Sci. Rev. **199**, 102 [illegible] (201[illegible]).
34. [illegible] J. Clim. **24**, 202 [illegible] –2044 (2011).
3[illegible]. [illegible] Nat. Hazards Earth Syst. Sci. **19**, 22[illegible]1–22[illegible] (201[illegible]).
3[illegible]. [illegible] Sci. Data **5**, 1[illegible] (201[illegible]).
3[illegible]. [illegible] Physiological Plant Ecology II: Water Relations and Carbon Assimilation ([illegible]). ([illegible] , 1[illegible]2).
3[illegible]. [illegible] Geophys. Res. Lett. **41**, [illegible] 013 (2014).
3[illegible]. [illegible] Planta **149**, [illegible] (1[illegible]0).
40. [illegible] Glob. Biogeochem. Cycles **23**, [illegible] (200[illegible]).
41. [illegible] Glob. Change Biol. **23**, [illegible] (201[illegible]).
42. [illegible] J. Exp. Bot. **66**, 43[illegible]–43[illegible]1 (201[illegible]).
43. [illegible] Environ. Res. Lett. **13**, 0[illegible]401[illegible] (201[illegible]).
44. [illegible] J. Geophys. Res.: Atmos. **125**, 2020[illegible]0330[illegible] (2020).
4[illegible]. [illegible] Glob. Change Biol. **22**, 404[illegible]–40[illegible] (201[illegible]).
4[illegible]. [illegible] Aquat. Bot. **86**, 10[illegible]–11[illegible] (200[illegible]).
4[illegible]. [illegible] Glob. Biogeochem. Cycles **18**, [illegible] 2004 (2004).
4[illegible]. [illegible] Oecologia **108**, 3[illegible]–4[illegible] (1[illegible]).
4[illegible]. [illegible] Glob. Ecol. Biogeogr. **30**, 3[illegible]–413 (2020).
[illegible]0. [illegible] Plant, Cell Environ. **22**, 1[illegible] (1[illegible]).
[illegible]1. [illegible] Catena **160**, 134–140 (201[illegible]).
[illegible]2. [illegible] Geosci. Model Dev. **15**, 4[illegible]0–4[illegible]3[illegible] (2022).
[illegible]3. [illegible] Glob. Change Biol. **26**, 411[illegible]–4133 (2020).
[illegible]4. [illegible] Sci. Total Environ. **806**, 1[illegible]0[illegible]31 (2022).
[illegible] [illegible] Q. J. R. Meteorol. Soc. **137**, [illegible] (2011).
[illegible] CRUNCEP Version 7 - Atmospheric Forcing Data for the Community Land Model. [illegible] /10.[illegible] 2021. (201[illegible]).
[illegible] [illegible] Sci. Data **9**, 40[illegible] (2022).
[illegible] [illegible] 2000-201[illegible] Sci. Data **4**, 1[illegible] (201[illegible]).
[illegible] [illegible] -2. Remote Sens. **11**, 2[illegible]3 (201[illegible]).
[illegible]0. [illegible] Nature **541**, 1[illegible]–20 (201[illegible]).
[illegible]1. [illegible] Numerical Terradynamic Simulation Group Publications. 2[illegible] (2013).
[illegible]2. [illegible] 2002–201[illegible]. Remote Sens. Environ. **222**, 1[illegible]–1[illegible]2 (201[illegible]).
[illegible]3. [illegible] Nat. Commun. **10**, 23[illegible] (201[illegible]).
[illegible]4. [illegible] Oecologia **164**, [illegible]–[illegible]0[illegible] (2010).
[illegible] [illegible] Hydrol. Process. **18**, 1[illegible]1–1[illegible] (2004).
[illegible] [illegible] Earth Syst. Sci. Data **12**, 121[illegible]–1243 (2020).

Acknowledgements

[illegible] 4222010400 [illegible] 4210110 [illegible] 422[illegible]1122 [illegible] 202201 [illegible] 4 [illegible] 2020 [illegible] 10 [illegible] 2022 1[illegible]0[illegible]44). [illegible] (214[illegible]130).

Author contributions

[illegible]

Competing interests

[illegible]

Additional information